Distance-Dependent Electronic Coupling at Molecule−Metal Interfaces: C_{60}/Cu(111)

Gregory Dutton and X.-Y. Zhu*

Department of Chemistry, University of Minnesota, Minneapolis, Minnesota 55455

Received: October 6, 2003; In Final Form: April 5, 2004

We probe electronic interaction at molecular-solid/metal interfaces in the model system of C_{60}/Cu(111) using femtosecond two-photon photoemission (2PPE) spectroscopy. The second lowest unoccupied molecular orbital (LUMO+1) and the LUMO+2 levels in C_{60} are transiently populated via the creation of electronic excitons, with lifetimes in the $10^{-14}-10^{-13}$ s region, likely due to self-trapping and/or decay into lower-lying exciton states. These lifetimes decrease as film thickness decreases. The effect is seen for films as thick as 50 Å and is attributed to quenching via charge transfer between the Cu substrate and electronic bands in C_{60}. The rates of quenching are found to depend exponentially on film thickness, with a β value of 0.11 ± 0.02 Å^{-1} for both LUMO+1 and the LUMO+2 levels.

1. Introduction

It is now well-recognized that the nature of the molecule−metal interface is one of the key factors governing the performance of molecular−semiconductor devices, such as organic light emitting devices, field-effect transistors and solar cells. Electronic interaction at such an interface is responsible for charge injection from an electrode to the molecular film. The efficiency or rate of injection is determined by (1) the energetic alignment of molecular orbitals to the metal Fermi level, and (2) the electronic coupling strength (wave function mixing) between molecular orbitals and metal bands. While energetic alignment has been probed by photoemission spectroscopies, electronic coupling strength at molecule−metal interfaces remains largely unknown at the present time. We attempt to address electronic coupling at molecule−metal interfaces, particularly the distance dependence, using the model system of C_{60}/Cu(111) and the experimental technique of time-resolved two-photon photoemission (TR-2PPE) spectroscopy.[1,2] The model is chosen because C_{60} is the most extensively studied and best understood system among all molecular solids. The wealth of information[3−5] on the electronic and optical properties of C_{60} from extensive experiment and theory allows a reliable and quantitative interpretation of 2PPE results. The C_{60}/Cu(111) interface is well-known to be highly ordered. C_{60} grows epitaxially on Cu(111), forming a (4×4) superlattice at the interface with lattice parameter only 1.7% larger than that in solid C_{60}.[6−9] There is charge transfer of 1.5−2 electrons from the Cu substrate to each C_{60} molecule within the first monolayer (ML). All C_{60} molecules in the second layer and beyond remain neutral and are nearly indistinguishable in 2PPE spectroscopy.[10]

Details on 2PPE spectroscopy of the C_{60}/Cu(111) system have been published before.[10] These measurements revealed three main peaks due to C_{60}: the highest occupied molecular orbital (HOMO), an unoccupied molecular orbital (U_A) at 2.87 eV above HOMO, and a second unoccupied level (U_B) at 4.07 eV above HOMO. The presence of occupied vs unoccupied states in a 2PPE spectrum is easily distinguished on the basis of the dependence of peak position on photon energy.[10] We concluded that the initial optical excitation should be within the molecular film, rather than metal-to-molecule interfacial charge transfer. This conclusion was based on the observation that the 2PPE spectrum showed little change when the film coverage was increased from 2 to 40 ML. We have also carried measurements for C_{60} coverage well above 40 ML (or >320 Å) and observed no further change in the spectrum. If the initial excitation were a result of metal-to-molecule charge transfer, we would expect the probability of the excess electron to locate predominantly at the metal−molecule interface due to stabilization of the image potential. The mean-free-path of conduction electrons in C_{60} solid is believed to be of the size of each C_{60} molecule.[4] Wertheim et al. arrive at the same conclusion for photoemitted electrons in an ultraviolet photoemission study of alkali-fullerides.[11] For such a short mean-free-path, the 2PPE signal from an interfacial charge-transfer mechanism should diminish rapidly with increasing coverage. As a result, the relative intensity of a 2PPE signal from the LUMO+1 or LUMO+2 level as referenced to that from the HOMO should decrease significantly with increasing film thickness. Even if we assume an order of magnitude increase in mean-free-path, as suggested by the universal curve, we should still expect a significant and observable change in the relative peak intensities when the C_{60} coverage is increased from 2 to 40 ML. These were not observed. Thus, we *exclude* the possibility of metal-to-molecule charge transfer as a mechanism for the population of the LUMO+1 and the LUMO+2 levels.

For an initial optical excitation within the C_{60} thin film, there are two possibilities for the assignment of the two unoccupied levels. The first possibility is to assign U_A and U_B as the lowest unoccupied molecular orbital (LUMO) and the LUMO+1 level, respectively, as done in our previous publication.[10] Within such an assignment, the HOMO−LUMO gap from 2PPE measurement is 2.87 eV, as compared to the 3.6 eV transport gap obtained from one-photon photoemission (PE) for HOMO and inverse photoemission (IPE) for LUMO.[12,13] Both PE and 2PPE should give the same value for the HOMO involving a one-hole final state. The situation is different for the LUMO: 2PPE yields a one-hole final state, while IPE gives a one-electron final state. If we assume the same electronic polarization energy for a hole and an excess electron in solid C_{60}, the lowering of

* Author to whom correspondence should be addressed. E-mail: zhu@chem.umn.edu.

10.1021/jp036996s CCC: $27.50
Published on Web 05/07/2004

0.7 eV of the LUMO seen in a 2PPE process can be attributed to stabilization of the transient electron by the presence of a hole. In other words, the initial optical excitation in 2PPE creates an exciton. However, this cannot be a HOMO−LUMO Frenkel (or on-molecule) exciton. The Frenkel exciton stabilization energy is 1.4−1.6 eV, the so-called Hubbard U.[12−14] Indeed, Long et al. showed that photoionization from a Frenkel exciton puts the LUMO peak at ∼2 eV above that of the HOMO peak.[15,16] Thus, if we assign U_A as the LUMO, it should be a charge-transfer exciton, or band-to-band transition with excitonic stabilization. The difference in stabilization energy for a Frenkel and a charge-transfer exciton can be simply attributed to the different electron−hole distance. The energetics, E^{CT}, of a charge-transfer exciton can be approximated by[17,18]

$$E^{CT} = I - A - 2P + C(r) \tag{1}$$

with

$$I - A - 2P = E_g^{Tr} \tag{2}$$

and

$$C(r) = -\frac{e^2}{\epsilon r} - \Delta P_{eh}(r) \tag{3}$$

where I and A are the ionization potential and electron affinity, respectively, of a single C_{60} molecule; P is the polarization energy of an electron or hole in solid C_{60}; $(I - A - 2P)$ is essentially the transport gap, E_g^{Tr}, determined from PE and IPE; $C(r)$ is the Coulomb interaction between an electron and a hole at distance r, and ϵ is the apparent dielectric constant; $\Delta P_{eh}(r)$ is a correction to the polarization energy $2P$ for the electron−hole pair at a finite distance r. These calculations gave the E^{CT} value of 2.65−2.90 eV (depending on the level of approximation) for the first charge-transfer exciton state with electron and hole located on nearest-neighbor C_{60} molecules.[18] The HOMO−LUMO gap (peak-to-peak) of 2.87 eV determined by our 2PPE measurement is in agreement with the calculated values for the CT exciton at the lowest level of theory (2.90 eV) but is higher than that from the highest level theory (2.65 eV). An electroabsorption experiment suggested the first CT exciton in solid C_{60} at 2.43 eV.[18] This value is also lower than the HOMO−LUMO gap from 2PPE. It is possible that the CT exciton probed in our 2PPE measurement may involve substantially delocalized character, i.e., exciton band. Note that, at the photon energy used in our study, the CT exciton may be created via the HOMO-2 → LUMO transition. On the basis of similar arguments, we may assign the U_B level as originating from a charge-transfer exciton, created via the HOMO-1 → LUMO+1 transition.

The second possibility is to assign U_A and U_B as the LUMO+1 and the LUMO+2 levels involved in Frenkel excitons. In fact, this was the assignment of an earlier 2PPE measurement of C_{60} films condensed on polycrystalline Cu or single-crystal Ag(100) by Eberhardt and co-workers, as detailed below.[19,20] It is known that the optical absorption spectrum of solid C_{60} is strikingly similar to that of isolated C_{60} molecules in the gas or solution phase, indicating that optical excitation in solid C_{60} is dominated by intramolecular excitations to form Frenkel excitons.[4] Oscillator strengths for exciton band or charge-transfer exciton transitions must be much lower than those of Frenkel excitons. The assignment of U_A and U_B as the LUMO+1 and LUMO+2 levels involved in Frenkel excitons is also supported by energetics: in C_{60} thin films, the HOMO → LUMO+1 ($h_u \rightarrow t_{1g}$) transition energy is 2.7−3.0 eV, while theory puts it at 2.86 eV.[4] This is in excellent agreement with our 2PPE value of 2.87 eV. The LUMO+2 level is known to be 1.2 eV above LUMO+1,[4,12] also in excellent agreement with our 2PPE measurement. On the basis of the excellent agreement in energetics and the oscillator strength argument, we favor the assignment of the observed U_A and U_B levels as LUMO+1 and LUMO+2 levels involved in Frenkel excitons. This calls for a modification of assignment in our previous publication.[10]

In earlier 2PPE measurements of C_{60} films, Eberhardt and co-workers also assigned spectral features at 2.2, 3.0, and 4.0 eV above the HOMO as the LUMO, the LUMO+1, and the LUMO+2 levels, respectively.[19,20] These two previous studies suffered from relatively low spectral resolution and intensity, due in part to the use of probe photon energy (6.0 eV) exceeding the work function (∼4.9 eV) of the material. The presence of significant one-photon photoemission signal interfered with that from 2PPE and limited the laser power applicable. For example, for a 3 nm thin film of C_{60} on Ag(100), these experimental limitations were responsible for the low 2PPE signal which was barely above the background noise level.[20]

In the present study, we use TR-2PPE to measure the relaxation dynamics of the transiently populated LUMO+1 and LUMO+2 levels in epitaxial films of C_{60} on Cu(111). A number of significant improvements in the present study over previous work by Eberhardt and co-workers are noteworthy. First, the use of the Cu(111) substrate allows us to grow high-quality epitaxial films of C_{60}; we found that spectral resolution indeed improves for better quality films prepared by dosing at elevated temperatures.[10] Second, the use of photon energies below the surface work function avoids complications due to one-photon photoemission and allows us to improve signal-to-noise ratio by several orders of magnitude. Third, the use of a tunable laser source allows us to unambiguously establish the occupied and unoccupied origin of the 2PPE signal.[10] These improvements allow us to quantitatively establish the distance-dependence of excited-state lifetimes and the rates of quenching by the metal substrate. Such quantitative evaluation of quenching rates on the distance to the metal surface is the focus of the present paper.

Note that the use of photon energies ≤4.9 eV in the present study prohibits us from observing the first Frenkel exciton involving the LUMO. For the Frenkel exciton, the LUMO lies at ∼2.2 eV above the HOMO, i.e., slightly above the Fermi level. Ionization from the LUMO level within the transient Frenkel exciton would put the electron kinetic energy at ∼0 eV only with the highest photon energy used (4.9 eV). Even at the highest photon energy used, a photoelectron from the Frenkel exciton could not be resolved from the secondary electron threshold. Thus, the present study relies on the LUMO+1 and LUMO+2 levels as probes of the distance-dependent quenching dynamics.

2. Experimental Section

All experiments were carried out in an ultrahigh vacuum (UHV) chamber with a base pressure of 7×10^{-11} Torr. The Cu(111) surface was cleaned by standard procedures. Details on the preparation of high-quality C_{60} epitaxial films on Cu(111) and the calibration of surface coverage by low-energy electron diffraction (LEED) and Auger electron spectroscopy (AES) were presented in our previous publication.[10] All coverages were referenced to a saturated monolayer (ML) which gave a sharp (4×4) LEED pattern.

The two-photon photoemission setup is shown in Figure 1. Laser light was generated by a Ti:sapphire oscillator (Coherent

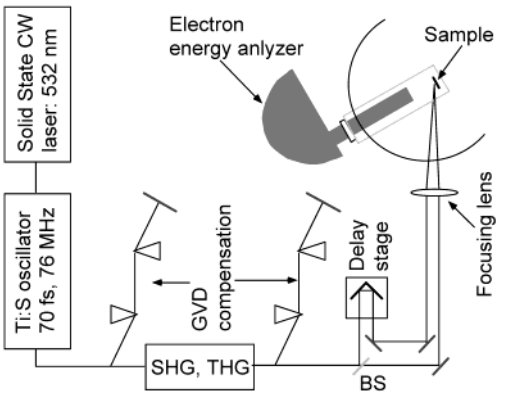

Figure 1. Experimental setup.

MIRA 900) pumped by an 8 W CW solid-state laser at 532 nm (Coherent Verdi-V8). The tunable wavelength Ti:sapphire fundamental (76 MHz, 0.8−1.5 W, 700−900 nm, ≤70 fs) was frequency tripled in an ultrafast harmonic generator package (INRAD 5-050) to obtain photon energies from 4 to 5 eV. Prism pairs, SF10 glass for the fundamental and UV fused silica for the harmonics, were used for dispersion compensation both before and after harmonic generation. The UV light was split into two beams (pump and probe) with equal intensity by a beam splitter (BS). The probe beam passed through a delay stage and recombined with the pump beam. Both pump and probe beams, p-polarized and incident at 60° from the spectrometer axis (normal to the sample surface), were brought to a 60−70 μm focus at the sample surface by an $f = 50$ cm focusing lens. An auto-correlation measurement using two-photon photoemission features from occupied states gave a pulse width of 69 ± 3 fs at $h\nu = 4.90$ eV.

Photoelectrons were detected with a hemispherical electron energy analyzer (Vacuum Generators 100AX) with an instrumental resolution of 35 meV, determined by fitting the Fermi edge of the cooled copper sample with an instrumentally broadened Fermi-Dirac distribution. This experimental broadening is dominated by the bandwidth of the laser pulses. The sample was oriented normal to the spectrometer for all measurements. Typical laser pulse fluence was ≤1 mJ/cm^2, and no evidence of space−charge effects was observed at this fluence level. The sample temperature was kept at 100 K in all measurements. There was no photopolymerization at this temperature,[21] and we observed no changes in 2PPE spectra with the extent of laser irradiation.

3. Results and Dicussions

The cartoon in Figure 2 illustrates the principle of a 2PPE experiment. The first photon ($h\nu_1$, pump) excites an electron from an occupied orbital to an unoccupied C_{60} orbital, and the second photon ($h\nu_2$, probe) ionizes the electron from the transiently populated orbital for detection. In spectroscopic mode, the first and second photons come from the same laser pulse; in time-resolved measurement, the two photons are from two time-delayed pulses. Details on spectroscopy in this system have been presented elsewhere,[10] but the assignment of the LUMO+x levels may be debatable, as discussed in the Introduction section. We adopt the new assignment in the present paper. The inset in Figure 2 shows a typical 2PPE spectrum taken at $h\nu = 4.90$ eV for 11 ML C_{60}/Cu(111). There are three main peaks in this spectral region: the highest occupied molecular orbital (HOMO), the LUMO+1 level at 2.87 eV above HOMO, and the LUMO+2 level at 4.07 eV above HOMO. Spectra taken at other C_{60} coverages ≥2 ML are nearly

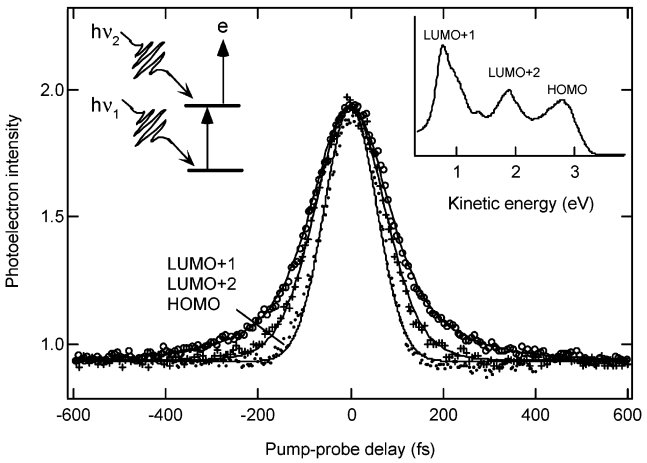

Figure 2. Pump−probe cross correlation curves of the HOMO (dots), LUMO+1 (crosses), and LUMO+2 (circles) from 11 ML C_{60}/Cu(111). The solid lines are fits, as detailed in the text. Inset: 2PPE spectrum from 11 ML C_{60}/Cu(111).

identical.[10] Note that on a kinetic energy scale, the HOMO peak is located above the LUMO+1 or LUMO+2 peak. This is because for 2PPE involving an unoccupied state, the initial state could be lower in energy (e.g., HOMO-1 or HOMO-2).

The lifetimes of electronic excitons in C_{60}/Cu(111) are established in cross correlation (CC) measurements, Figure 2. In these experiments, photoelectron signal at each peak in the spectrum (inset) is recorded as a function of pump−probe delay time. CC traces from the LUMO+1 and LUMO+2 peaks are clearly broader than that from the HOMO. The analysis of cross correlation data in TR-2PPE has been well established in previous work.[22,23] Briefly, for two-photon ionization from an occupied state without the population of an intermediate state, the optical fields from the two laser pulses add coherently, and the CC trace is essentially an auto-correlation (AC) curve on top of a constant background due to signals from two individual laser pulses. For two-photon ionization via an intermediate state, which can decay with a finite lifetime, the CC trace consists of three components: (1) a coherent component (also called coherent artifact) which results from the fact that the optical fields from both laser pulses add coherently and enhance transition probabilities in both excitation steps; (2) an incoherent component which reflects the dynamics of the transiently populated intermediate state; and (3) the constant background. In principle, the intensity ratio at zero time-delay is 1:1:1 for the three components.[23] In practice, the background signal is usually higher because the spatial overlap of the two laser pulses is less than 100%.

Because a 2PPE signal from the HOMO involves coherent two-photon ionization via a virtual intermediate state, this trace is taken as an auto-correlation (AC) trace. Measurement of the occupied surface state on clean Cu(111) shows CC traces nearly identical to that from the C_{60} HOMO. Fitting the HOMO cross-correlation data to the well-known Gaussian or hyperbolic sech functions[24] gives a pulse width of $\tau_{pulse} = 90 \pm 5$ or 70 ± 3 fs, respectively. Within noise level, we found no difference in fitting quality using these two AC functions. The dashed curve on top of the data (dots) shows a typical fit, which satisfactorily describes the experimental data.

Cross-correlation curves from the LUMO+1 (crosses) and the LUMO+2 (circles) peaks are broader than the AC function, indicating finite lifetimes for these transiently populated levels. If we assume a single-exponential decay with lifetime of τ_{life}, the experimental CC data above the constant background can

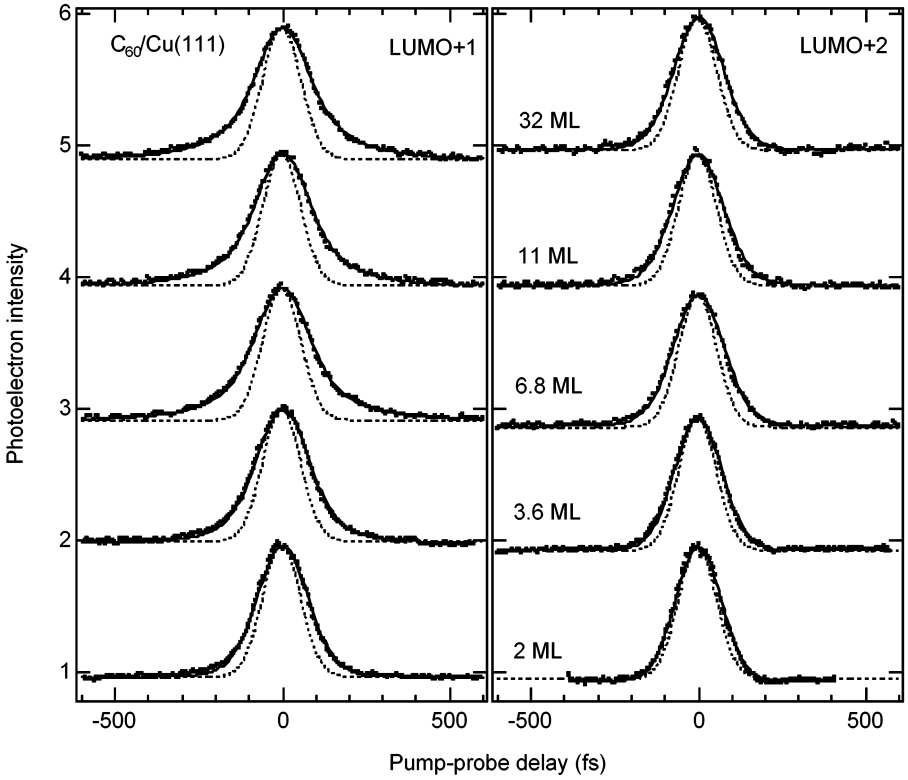

Figure 3. Pump−probe cross correlation (dots) of the LUMO+2 (right) and LUMO+1 (left) levels in C_{60}/Cu(111) at the indicated coverages (2−32 ML). The solid lines are fits as described in the text. The dashed lines are the auto-correlation curves determined from cross-correlation of the HOMO. All curves are normalized with respect to the peak intensities.

be described by the sum of the AC function (coherent artifact), S_{AC}, and the incoherent component, S_{inc}, which is a convolution of the AC function and a symmetric exponential decay function (on both sides of t = zero):

$$S_{inc}(\tau) \propto \int_{-\infty}^{\infty} S_{AC}(t-\tau)e^{-|t|/\tau_{life}}\,dt \qquad (4)$$

where τ is the pump−probe delay and S_{AC} is the auto-correlation function. In the least-squares fitting process, we keep the peak intensity ratio between S_{AC} and S_{inc} as a constant of 1:1. The resulting fits (solid curves) are in excellent agreement with experimental data and give lifetimes of $\tau_{life} = 114 \pm 5$ and 45 ± 5 fs for the LUMO+1 and the LUMO+2 peaks, respectively.

We carry out cross-correlation measurements for the LUMO+1 and the LUMO+2 levels as a function of C_{60} film thickness, Figure 3. A comparison of each cross-correlation curve with the auto-correlation curve (dashed lines) clearly shows an increase in excited-state lifetime with increasing film thickness. The solid lines are fits to $S_{AC}+S_{inc}$, as described above. The results of the fitting are summarized as a function of film thickness in Figure 4. The solid lines are fits to a simple exponential function. The asymptotic values are 116 ± 5 fs and 45 ± 5 fs for the LUMO+1 and LUMO+2 levels, respectively.

Before addressing the coverage dependence of these ultrafast dynamic processes, we first discuss the dynamics in bulk C_{60}. As shown in Figure 4, for C_{60} coverages > 6 ML, the decay dynamics of both LUMO+1 and LUMO+2 levels are independent of film thickness and must be attributed to intrinsic mechanisms in solid C_{60}. The value of $\tau_{life} = 116$ fs for the LUMO+1 level in bulk C_{60} is lower than the previously reported value of 268 fs for the same level in thick C_{60} films on Ag(100).[20] This difference may be attributed to the different excitation photon energies used: 3 eV in the work of Eberhardt and co-workers and 4.9 eV in the present study. Difference in initial excitation energy can lead to not only different energetic location of the transient hole within the exciton, but also different degrees of vibronic excitation within the Franck−Condon envelope. Note that the LUMO+2 level labeled here (4.07 eV above HOMO) was not accessible energetically (in the excitation step) in the previous work on Ag(100). Note also that the LUMO level in the previous work is not observed here due to the lower probe photon energy used. The first Frenkel exciton (HOMO → LUMO) decays on a much longer time scale (130 ps for the singlet and 1 ns for the triplet).[20]

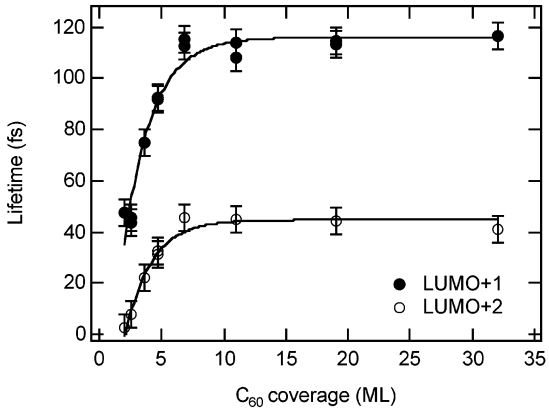

Figure 4. The dependences on film thickness of transient lifetimes for the LUMO+1 (solid circles) and LUMO+2 (open circles) levels. The solid lines are exponential fits.

There have been a large number of studies on ultrafast dynamics in thin films and crystalline fullerenes.[25−35] Most of these experimental results revealed dynamic processes on relatively longer time scales than those shown in Figure 4. For example, an extensively studied process is exciton annihilation which occurs on a picosecond time scale and is strongly dependent on excitation density (laser power).[25] While we did

not carry out extensive studies on power dependence, we observed no change in cross-correlation results for changes in laser power within a factor of 2. The ultrafast decays of LUMO+1 and LUMO+2 levels are believed to be of different origins. The exact mechanism of such ultrafast decay is not known, but we can identify several possibilities. Following the initial photoexcitation to form an electronic exciton, electron−nuclear interaction can lead to the formation of a polaron-exciton, also called a self-trapped exciton. The formation of self-trapped excitons can occur on an ultrafast time scale, i.e., the inverse of the vibrational frequency involved. There are indeed a number of intramolecular vibrations and phonon modes around these lifetime values.[36−38] Such a self-trapping process does not lead to significant decrease in the energetic position of the electron in the LUMO+1 or LUMO+2 level, but may result in a substantial change (decrease) in the transition dipole moment for photoionization, thus a decrease in 2PPE single seen here. In addition to the self-trapping process, the exciton state involving LUMO+1 and LUMO+2 levels can also rapidly decay into lower-lying states, e.g., the Frenkel exciton involving the LUMO. It is therefore not surprising that exciton lifetimes involving the LUMO+1 and LUMO+2 levels are much shorter than that for the LUMO level. Note that, once self-trapped, the polaron-exciton decays on much slower time scales, but these slow processes are not probed in the present experiment. In the following, we focus on one issue: quenching of these electronic excitons by the metal substrate.

For both the LUMO+1 and the LUMO+2 levels, the lifetimes decrease with decreasing film thickness for C_{60} coverage ≤ 6 ML or film thickness ≤ 50 Å. Both lifetimes decrease exponentially with decreasing film thickness, with nearly identical functional dependences. Previous work on Ag(100) also noted a decrease in the LUMO+1 lifetime for film thickness less than 6 nm.[20] To understand these coverage dependences, we first establish the origin of photoemission signal from a multilayer C_{60} film. As shown previously, while the first layer of C_{60} molecules is negatively charged and give completely different 2PPE spectrum, spectra from C_{60} coverages of 2 ML and above are nearly identical.[10] We believe each 2PPE spectrum from a multilayer film is dominated by a contribution from the topmost layer of C_{60} molecules for the following reasons: (1) the intensity of 2PPE spectrum does not change significantly with increasing coverage. Any increase in intensity, if present, is within 20% when the surface coverage increases from 2 to 40 ML. This result indicates that the mean-free-path of nascent photoelectrons is very small in C_{60}, probably on the order of or smaller than the molecular diameter. The same conclusion has been made before for conduction electrons[4] or photoemitted electrons;[11] (2) With increasing C_{60} coverage (> 2 ML), we see a small, but systematic shift in all peak positions.[10] However, there is no peak broadening as compared to that at 2ML coverage, indicating there is no significant mixing of signal from different layers of C_{60} molecules.

What is the mechanism of this substrate-mediated quenching channel? For an electronically excited state near a metal surface, a universally present quenching channel is dipole and induced-dipole coupling, i.e., Foerster energy transfer. However, the rate of such a dipole channel is not high enough to give sub 100 fs lifetimes.[39] A much more efficient channel is charge transfer between the excited molecule and the metal substrate. Such a charge-transfer mechanism is well established in the extensive literature of photochemistry on metal surfaces.[40] The femtosecond time scales for electron transfer between adsorbed molecules and metal substrates have been established by indirect

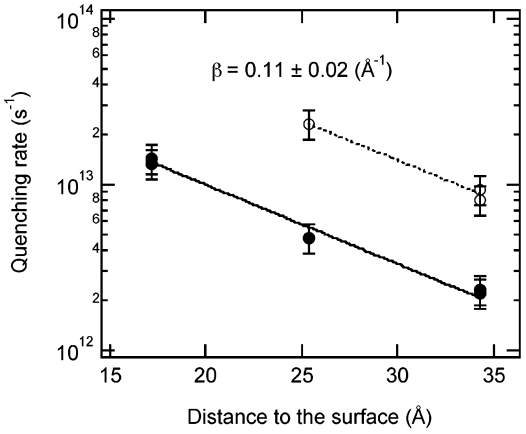

Figure 5. The dependences of substrate quenching rates for the LUMO+1 (solid circles) and LUMO+2 (open circles) levels as a function of distance to the Cu(111) surface. The solid and dotted lines are fits to eq 7, which yield the indicated β value.

measurements on surface photochemical cross sections, isotope effects, and final state distributions,[40] as well as direct measurements by time-resolved 2PPE.[41] For example, the lifetime of transiently populated LUMO in hexafluorobenzene on Cu(111) was found to be 15−50 fs (depending on coverage) due to strong coupling between the LUMO band and unoccupied Cu states.[41] Efficient electron transfer between donor molecules and photoexcited C_{60} is also well-known in solution-phase studies.[42,43] Quenching of an electronic exciton in the C_{60} film by the Cu substrate may occur via the transfer of the transient electron in a LUMO+1 or LUMO+2 orbital to unoccupied metal bands above the Fermi level, as well as the filling of photogenerated hole in C_{60} by a Cu electron below the Fermi level.

We can semiquantitatively establish the distance dependence in quenching rates. At an intermediate coverage (≤6 ML), the decay rate from each state can be approximated by the sum of two relaxation channels: an intrinsic rate, $1/\tau_{in}$, where τ_{in} is 116 or 45 fs for the LUMO+1 or LUMO+2, respectively, and an external quenching rate, k_q, due to charge transfer to the Cu substrate:

$$\frac{1}{\tau_{life}} = \frac{1}{\tau_{in}} + k_q \tag{5}$$

The substrate quenching rates obtained from eq 5 are shown as a function of distance to the metal surface in Figure 5. Here, distance to the surface (from the center of each C_{60} molecule in the topmost layer) is converted from coverage based on the bulk value of 8.17 Å for distance between (111) planes in crystalline solid C_{60}. In each case, only lifetime values significantly below the asymptotic values but above 10 fs (limit of time resolution from fitting) are used. In electron-transfer literature, distance-dependence in electron-transfer rate (k_{ET}) is often described by exponential functions of the form

$$k_{ET} = k_o e^{-\beta d} \tag{6}$$

where the β parameter (Å^{-1}) characterizes the nature of the bridge in mediating electron transfer within a tunneling picture. Despite the limited number of data points in Figure 5, quenching rates for both LUMO+1 and LUMO+2 levels can be described by eq 6 with a common β value of 0.11 ± 0.02 Å^{-1}. The β observed here is significantly smaller than typical values for tunneling through molecular bridges. For comparison, the β values in molecular bridges range from the lowest value of 0.2

$Å^{-1}$ in π-conjugated molecules to 1.0 $Å^{-1}$ in saturated alkyls.[44] The k_o values from the fits in Figure 5 are 9.0×10^{13} and 3.6×10^{14} s^{-1} for the LUMO+1 and LUMO+2 levels, respectively. These rate constants for quenching at zero distance correspond to electronic coupling strengths of $\Gamma = 0.06$ and 0.24 eV for the LUMO+1 and LUMO+2 levels, respectively, as estimated from the uncertainty principle ($\Gamma \approx \hbar \cdot k_o$).

Both the large k_o and the small β values suggest strong electronic coupling. Thus, it is inadequate to describe charge transfer between electronic excitons in C_{60} and the Cu substrate as tunneling. Instead, one should view ultrafast charge transfer between the topmost molecular layer and the Cu substrate as due to direct electronic coupling, mediated by delocalized electronic bands. Theoretical studies predict bandwidths of 400−600 meV for exciton bands in solid C_{60}.[4,36] We carried out angle-resolved measurements but did not observe appreciable amounts of dispersion.[10] However, small dispersion with bandwidth on the order of ∼100 meV may not be observable given the fact that the width of the LUMO+1 or LUMO+2 peak in the 2PPE spectrum is ∼0.5 eV.

Accepting such a substrate-mediated, charge-transfer quenching channel, we can understand the coverage dependence as follows. With increasing C_{60} thickness, $|\Psi|^2$ within a delocalized C_{60} band is, on average, farther away from the Cu surface; as a result, its coupling (wave function mixing) with the Cu substrate decreases. At coverages >6 ML, the charge-transfer quenching mechanism cannot compete with the intrinsic lifetimes within solid C_{60}. Another way of looking at the result is that, as far as dynamics is concerned, the metal−molecule contact effect is confined to a thickness of ∼6 monolayers of C_{60} molecules.

4. Conclusions

The ultrafast relaxation dynamics of excitons in C_{60} epitaxial films on Cu(111) have been probed by femtosecond two-photon photoemission (2PPE) spectroscopy. The LUMO+1 and the LUMO+2 levels in C_{60} are transiently populated via the creation of electronic excitons, with lifetimes in the 10^{-14}−10^{-13} s region, likely due to self-trapping processes to form polaron-excitons and/or decay into lower-lying exciton states. These lifetimes decrease as film thickness decreases, an effect which is attributed to efficient charge transfer between electronic exciton bands in C_{60} and the Cu substrate. The rate of charge transfer between the excitons in C_{60} and the Cu substrate is found to depend exponentially on distance, with a β value of 0.11 ± 0.02 $Å^{-1}$.

Acknowledgment. This work was supported by the National Science Foundation through Grants DMR 9982109, 0238307, and by the MRSEC Program under Award Number DMR-0212302.

References and Notes

(1) Petek, H.; Ogawa, S. *Annu. Rev. Phys. Chem.* **2002**, *53*, 507.
(2) Harris, C. B.; Ge, N.-H.; Lingle, R. L., Jr.; McNeil, J. D.; Wong, C. M. *Annu. Rev. Phys. Chem.* **1997**, *48*, 711.
(3) *Optical and Electronic Properties of Fullerenes and Fullerene-based Materials*; Shinar, J., Vardeny, Z. V., Kafafi, Z. H., Eds.; Marcel Dekker: New York, 2000.
(4) Dresselhaus, M. S.; Dresselhaus, G.; Eklund, P. C. *Science of Fullerenes and Carbon Nanotubes*; Academic Press: New York, 1996.
(5) *Fullerenes: Chemistry, Physics, and Technology*; Kadish, K. M., Ruoff, R. S., Eds.; John Wiley & Sons: New York, 2000.
(6) Rowe, J. E.; Rudolf, P.; Tjeng, L H.; Malic, R. A.; Meigs, G.; Chen, C. T.; Chen., J.; Plummer, E. W. *Int. J. Mod. Phys.* **1992**, *6*, 3909.
(7) Tsuei, K.-D.; Johnson, P. D. *Solid State Commun.* **1997**, *101*, 337.
(8) Tsuei, K.-D.; Yuh, J.-Y.; Tzeng, C.-T.; Chu, R.-Y.; Chung, S.-C.; Tsang, K.-L. *Phys. Rev. B* **1997**, *56*, 15412.
(9) Hoogenboom, B. W.; Hesper, R.; Tjeng, L. H.; Sawatzky, G. A. *Phys. Rev. B* **1998**, *57*, 11939.
(10) Dutton, G.; Zhu, X.-Y. *J. Phys. Chem. B* **2002**, *106*, 5975.
(11) Wertheim, G. K.; Buchanan, D. N. E.; Chaban, E. E.; Rowe, J. E. *Solid State Commun.* **1992**, *83*, 785
(12) Weaver, J. H. *J. Phys. Chem. Solids* **1992**, *53*, 1433.
(13) Rudolf, P.; Golden, M. S.; Bruhwiler, P. A. *J. Electron Spectrosc. Relat. Phenom.* **1999**, *100*, 409.
(14) Lof, R. W.; van Veenendaal, M. A.; Koopmans, B.; Jonkman, B.; Sawatzky, G. A. *Phys. Rev. Lett.* **1992**, *68*, 3924.
(15) Long, J. P.; Chase, S. J.; Kabler, M. N. *Phys. Rev. B* **2001**, *64*, 205415.
(16) Long, J. P.; Chase, S. J.; Kabler, M. N. *Chem. Phys. Lett.* **2001**, *347*, 29.
(17) Munn, R. W. *Mol. Phys.* **1988**, *64*, 1.
(18) Kazaoui, S.; Minami, N.; Tanabe, Y.; Byrne, H. J.; Eilmes, A.; Petelenz, P. *Phys. Rev. B* **1998**, *58*, 7689.
(19) Jacquemin, R.; Kraus, S.; Eberhardt, W. *Solid State Commun.* **1998**, *105*, 449.
(20) Link, S.; Scholl, A.; Jacquemin, R.; Eberhardt, W. *Solid State Commun.* **2000**, *113*, 689.
(21) Itchkawitz, B. S.; Long, J. P.; Schedel-Niedrig, T.; Kabler, M. N.; Bradshaw, A. M.; Schlögl, R.; Hunter, W. R. *Chem. Phys. Lett.* **1995**, *243*, 211.
(22) Ogawa, S.; Petek, H. *Surf. Sci.* **1996**, *357*−*358*, 585.
(23) Knoesel, E.; Hotzel, A.; Wolf, M. *Phys. Rev. B* **1998**, *57*, 12812.
(24) Reid, G. D.; Wynne, K. *Encyclopedia of Analytical Chemistry: Instrumentation and Applications*; Meyers, R. A., Ed.; John Wiley & Sons: Chichester, 2000; pp 13644−13670.
(25) Dexheimer, S. L. In *Optical and Electronic Properties of Fullerenes and Fullerene-based Materials*; Shinar, J., Vardeny, Z. V., Kafafi, Z. H., Eds.; Marcel Dekker: New York, 2000; page 21 and references therein.
(26) Cheville, R. A.; Halas, N. J. *Phys. Rev. B* **1992**, *46*, 7329.
(27) Brorson, S. D.; Kelley, M. K.; Wenschuh, U.; Buhleier, R.; Kuhl, J. *Phys. Rev. B* **1992**, *46*, 7329.
(28) Flom, S. R.; Pong, R. G. S.; Bartoli, F. J.; Kafafi, Z. H. *Phys. Rev. B* **1992**, *46*, 15598.
(29) Farztdinov, V. M.; Lozovik, Y. E.; Matveets, Y. A.; Stepanov, A. G.; Letokhov, V. S. *J. Phys. Chem.* **1994**, *98*, 3290.
(30) Dick, D.; Wei, X.; Jeglinski, S.; Benner, R. E.; Vardeny, Z. V.; Moses, D.; Srdanov, V. I.; Wudl, F. *Phys. Rev. Lett.* **1994**, *73*, 2760.
(31) Janner, A.-M.; Eder, R.; Koopmans, B.; Jonkman, H. T.; Sawatzky, G. A. *Phys. Rev. B* **1995**, *52*, 17158.
(32) Nakamura, A.; Ichida, M.; Yajima, T.; Shinohara, H.; Saitoh, Y. *J. Lumin.* **1996**, *66*−*67*, 383.
(33) Ichida, M.; Nakamura, A.; Shinohara, H.; Saitoh, Y. *Chem. Phys. Lett.* **1998**, *289*, 579.
(34) Ishihara, S.; Ikemoto, I.; Suzuki, S.; Kikuchi, K.; Achiba, Y.; Kobayashi, T. *Chem. Phys. Lett.* **1998**, *295*, 475.
(35) Cho, H. S.; Yang, S. I.; Kim, S. K.; Shin, E.-j.; Kim, D. *J. Phys. Chem. B* **1999**, *103*, 6504.
(36) Dresselhaus, M. S.; Dresselhaus, G.; Eklund, P. C.; Saito, R. In *Optical and Electronic Properties of Fullerenes and Fullerene-based Materials*; Shinar, J., Vardeny, Z. V., Kafafi, Z. H., Eds.; Marcel Dekker: New York, 2000; page 217.
(37) Akselrod, L.; Byrne, H. J.; Donovan, S.; Roth, S. *Chem. Phys.* **1995**, *192*, 307.
(38) Coulombeau, C.; Jobic, H.; Bernier, P.; Fabre, C.; Schultz, D.; Rassat, A. **1992**, *96*, 22.
(39) Chance, R. R.; Prock, A.; Silbey, R. *Adv. Chem. Phys.* **1978**, *37*, 1.
(40) Zhu, X.-Y. *Annu. Rev. Phys. Chem.* **1994**, *45*, 113.
(41) Zhu, X.-Y. *Annu. Rev. Phys. Chem.* **2002**, *53*, 221.
(42) Sun, Y.-P.; Riggs, J. E.; Guo, Z.; Rollins, H. W. In *Optical and Electronic Properties of Fullerenes and Fullerene-based Materials*; Shinar, J., Vardeny, Z. V., Kafafi, Z. H., Eds.; Marcel Dekker: New York, 2000; p 43.
(43) Guldi, D. M.; Kamat, P. V. In *Fullerenes: Chemistry, Physics, and Technology*; Kadish, K. M., Ruoff, R. S., Eds.; John Wiley & Sons: New York, 2000; p 225.
(44) Adams, D. M., et al. *J. Phys. Chem. B* **2003**, *107*, 6668.